

Enhancing Power Sharing Strategy for Consistent Decarbonized Energy Sources in DC Residential Microgrids

Hong Phuc Lam*, Non-member
Quang T. D. Pham**, Non-member

Thoi Hung Ly*, Non-member
Minh Duc Pham*, Non-member
Duc Hung Nguyen*,^a, Non-member

A key issue in the transition to decarbonized energy sources with constant power sources is inaccurate current sharing and voltage quality. The main reason which causes these issues is the inevitable system impedance mismatches. This study addresses this issue by proposing an enhanced power-sharing strategy that regulates adjustable resistance and compensates for voltage drops across the line impedance at the output of distributed generation converters. The control approach involves analyzing the mathematical relationship between system impedance mismatches and voltage drops in DC residential systems. Utilizing low-computation proportional-integral controllers, the secondary current sharing and load voltage controllers regulate converter outputs to compensate for mismatched resistance and voltage, ensuring proper current sharing and load voltage quality across various load conditions. Through the implementation of the proposed scheme incorporating adjustable resistance and voltage shifting terms, both the current-sharing error and load voltage deviation are gradually reduced to negligible values, while maintaining stable performance in steady-state conditions, without the need for prior knowledge of system parameters. Simulations and experimental studies are both conducted to demonstrate the effectiveness of the proposed control scheme. © 2024 Institute of Electrical Engineer of Japan and Wiley Periodicals LLC.

Keywords: DC residential microgrid; energy sharing; MATLAB/SIMULINK simulation; load power balancing

Accepted 16 May 2024

1. Introduction

Decarbonized energy sources are extremely important in lowering carbon emissions and mitigating the effects of climate change. Shifting to low-carbon energy alternatives addresses energy security challenges and enhances supply system resilience [1,2]. The integration of decarbonized sources in residential areas is difficult due to the decarbonized energy sources are distributed over a long distance [3]. Furthermore, compared to fossil energy sources, decarbonized energy sources have a smaller capacity, which needs an advantage control strategy to coordinate distributed generation converters [4]. A viable solution to this problem is the deployment of the DC microgrid (DC-MG), which offers an advantage in power coordination among distributed generation converters [5].

In DC microgrids, achieving accurate current sharing among sources and regulating the DC system voltage within an acceptable range are key control objectives. Inaccurate current sharing can lead to overloading, compromising system reliability, while poor

voltage regulation can result in power quality issues. Conventional voltage control using the droop technique, although simple to implement, is sensitive to line impedance, affecting current sharing accuracy and DC bus (or load) voltage quality [6].

To improve the load-sharing performance, the authors Prajof Prabhakaran *et al.* [7] proposed a novel nonlinear droop control technique. Based on the calculated current sharing error percentage, the high-droop gain is added to the droop control equation for voltage regulation. Although the power-sharing performance is improved; the polynomial droop curve is complex, and the load voltage quality is not yet considered.

To address voltage quality concerns, Mehdi *et al.* [8] proposed a voltage restoration scheme with the aid of an external central controller system. Another control scheme of author Peng *et al.* [9] aimed to reduce reliance on costly central controllers while enhancing load voltage quality. However, neither study addressed current sharing issues.

Conversely, the control approach in Ref. [10] of the author Lin *et al.* focused on improving current sharing performance but did not consider load voltage regulation. Also, the control scheme in Ref. [10] required prior knowledge of system parameters for piecewise parameter design. To overcome this issue, the authors Peyghami *et al.* [11] proposed a technique involving injecting an AC signal to estimate line impedance mismatches for accurate current sharing and load voltage improvement. However, this

^a Correspondence to: Duc Hung Nguyen. E-mail: hungnd@hcmut.edu.vn

*Power Electronics Research Laboratory, Faculty of Electrical and Electronics Engineering, Ho Chi Minh City University of Technology (HCMUT), VNU-HCM, Ho Chi Minh City, Vietnam

**Faculty of Transportation Engineering, Ho Chi Minh City University of Technology (HCMUT), VNU-HCM, Ho Chi Minh City, Vietnam

method's complexity, potential impact on system stability, and susceptibility to noise raise concerns. Furthermore, the sensor sensitivity should be high enough to detect the injected AC signal, and the controller parameters have to be carefully designed to inject the AC signal properly.

To address the aforementioned challenges, our paper proposes a simple enhancing power sharing scheme to reduce system complexity and extend control to multiple distributed DC-DC converters. The proposed scheme regulates virtual resistance and compensates for voltage drop on line impedance. It involves measuring load voltage and receiving output current from each converter, then transmitting error and load voltage to local controllers. Utilizing low-computation proportional–integral controllers, the secondary current sharing and load voltage controllers regulate output voltage to compensate for mismatched resistance and voltage, ensuring proper current sharing and load voltage quality across various load conditions. Through the implementation of the proposed scheme incorporating adjustable resistance and voltage shifting terms, both the current-sharing error and load voltage deviation are gradually reduced to negligible values, while its performance remains stable in steady-state conditions, without the need of prior knowledge of system parameter. Moreover, even in extreme scenarios such as doubling ($2\times$) or tripling ($3\times$) the load power ($R_{load_3} = R_{load_2} = R_{load_1}$), the proposed control scheme demonstrates consistent stability and reliability. The effectiveness of the proposed control scheme is verified through rigorous MATLAB/SIMULINK simulations, as well as through experimentation on a small-scale laboratory setup.

2. Analysis of the DC Residential Microgrid

Consider a DC microgrid comprising N generators and load. The DC-DC converter based generators and loads are interconnected in parallel and control the current transferred to the DC bus. Figure 1 shows the equivalent DC microgrid circuit with three DC-DC converters for simplified analysis.

The conventional control method yields a linear relationship for the output voltage of the i th converter [10]. This relationship is determined by the output voltage and the virtual resistance, and can be expressed as follows:

$$V_{o_i}^* = V_{nor_i} - I_{o_i} R_{Droop_i} \quad (i \in N) \quad (1)$$

where $V_{o_i}^*$ is the output voltage reference, $V_{nor_i} = V_{nor}$ is the normal voltage (or ideal voltage), I_{o_i} is the output current, and R_{Droop_i} is the fixed initial electrical resistance value of the i th converter. The impact of R_{line_1} and R_{Droop_1} on the output current I_{o_1} in per unit is shown in Fig. 2.

The initial resistance value (R_{Droop}), also known as the droop resistance, is employed to distribute current among the DC-DC converters. In this study, this value is assumed to be appropriate for the power converter ($R_{Droop_1} = R_{Droop_2} = R_{Droop}$), and it is selected in two cases: 0.5Ω and 1Ω . This selection is intended to emphasize the impact of output current and line impedance mismatches on the bus voltage drop (or voltage quality). The value of R_{Droop} is defined as

$$\begin{cases} R_{Droop} = 0.5\Omega : \text{low droop gain case} \\ R_{Droop} = 1\Omega : \text{high droop gain case} \end{cases} \quad (2)$$

By applying Kirchoff's current and voltage laws to the circuit in Fig. 1, with the assumption that $V_{o_i} = V_{o_i}^*$, the output current

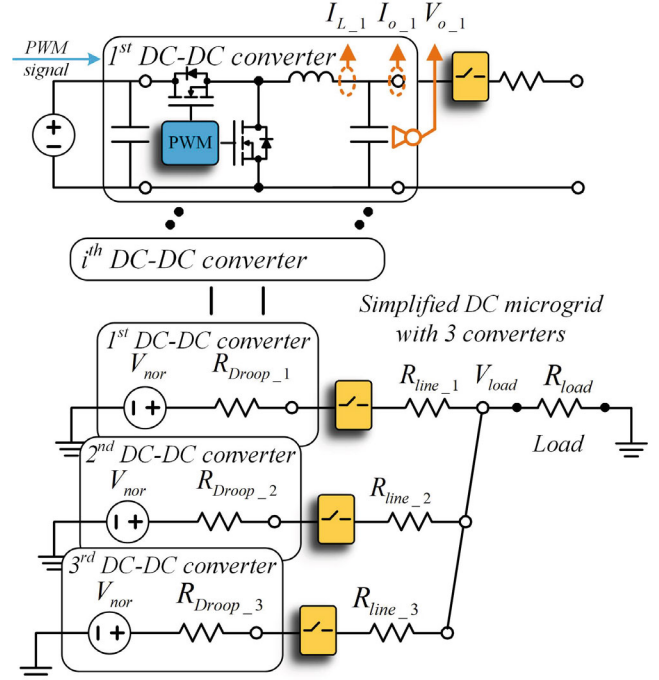


Fig. 1. Equivalent DC microgrid circuit with three DC-DC converters for simplified analysis

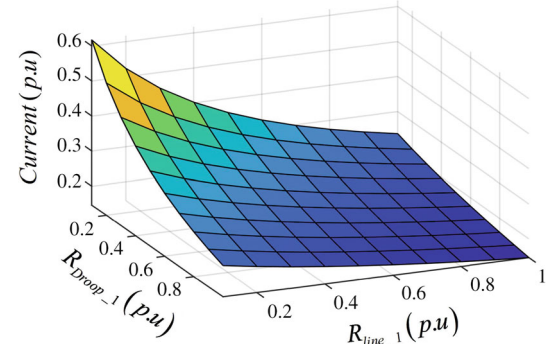


Fig. 2. Effect of line resistance on the output current of the converter

of each converter can be derived as

$$\begin{cases} I_{o_1} = \frac{R_{Comb_2}R_{Comb_3}V_{nor}}{R_{eq}}; I_{o_2} = \frac{R_{Comb_1}R_{Comb_3}V_{nor}}{R_{eq}}; \\ I_{o_3} = \frac{R_{Comb_1}R_{Comb_2}V_{nor}}{R_{eq}} \end{cases} \quad (3)$$

where R_{Comb_i} and R_{eq} are calculated as follows

$$\begin{cases} R_{Comb_i} = R_{Droop_i} + R_{line_i}, \forall i \in [1; 3] \\ R_{eq} = \left[\sum_{i=1}^3 (R_{Comb_i} + R_{load}) \right] R_{load}^2 - 2R_{load}^3 \\ \quad + \prod_{i=1}^3 (R_{Comb_i} + R_{load}) \end{cases} \quad (4)$$

The current sharing errors between 1st converter and j th converters ($j = 2, 3$) are calculated as

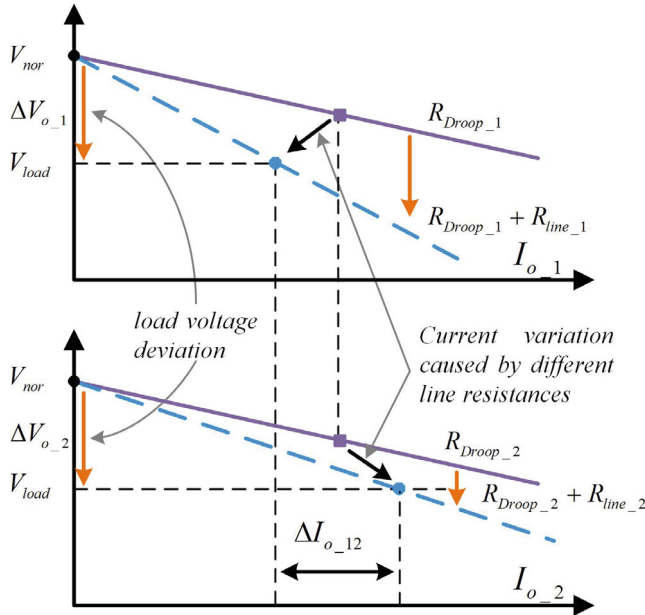


Fig. 3. The output voltage–current characteristic of 1st converter and 2nd converter

$$\begin{cases} \Delta I_{o_12} = I_{o_1} - I_{o_2} = (R_{Comb_2} - R_{Comb_1}) R_{Comb_3} V_{nor} / R_{eq} \\ \Delta I_{o_13} = I_{o_1} - I_{o_3} = (R_{Comb_3} - R_{Comb_1}) R_{Comb_2} V_{nor} / R_{eq} \end{cases} \quad (5)$$

By using the (5), the current sharing error of the 1st converter is defined as

$$\begin{aligned} \Delta I_{o_1} &= \Delta I_{o_12} + \Delta I_{o_13} \\ &= \frac{[(R_{Droop_3} + R_{line_3}) - (R_{Droop_1} + R_{line_1})] [(R_{Droop_2} + R_{line_2}) V_{nor}]}{R_{eq}} \\ &\quad + \frac{[(R_{Droop_2} + R_{line_2}) - (R_{Droop_1} + R_{line_1})] [(R_{Droop_3} + R_{line_3}) V_{nor}]}{R_{eq}} \end{aligned} \quad (6)$$

Figure 3 depicts the output voltage–current characteristic of the 1st and 2nd converters. Since the line impedance is typically unknown in practical applications, one possible approach to directly regulate the output current is by controlling the value of R_{Droop_i} ($i = 1, 2, 3$). To mitigate current sharing error in (5) and (6), it is essential to propose an additional controllable resistance into R_{Droop_i} .

In addition to the current sharing issue, the deviation in load voltage is also a significant concern. By analyzing the circuit in Fig. 1, the load voltage deviation can be determined using the following expression:

$$\begin{aligned} \Delta V_{o_1} &= V_{nor} - V_{load} = I_{o_1} (R_{Droop_1} + R_{line_1}) \\ &= R_{Comb_1} R_{Comb_2} R_{Comb_3} V_{nor} / R_{eq} \end{aligned} \quad (7)$$

Since all terms in the (7) are positive, the occurrence of load voltage deviation is unavoidable, especially with an increase in load current. (7) suggests that one viable solution to address the voltage drops issue is to integrate a voltage shifting term into the converter's voltage control loop.

3. Principle of the Proposed Control Method

3.1. Proposed coordinated adjustable impedance and voltage shifting

To solve the drawbacks of the conventional control scheme, a coordinated adjustable impedance

and voltage shifting terms are proposed regardless of the prior knowledge of system parameter. Figure 4 shows block diagram of the proposed control scheme with physical layer and digital layer. The physical layer includes power DC-DC circuits, sensor locations, and PWM control signals. The digital layer control layer includes detailed algorithm block diagrams corresponding to the converter's controller, which are divided into four parts. The roles and functions of each part are briefly explained below.

In the first part of the system, labeled “Voltage Measurement and Current Error Calculation” the power converter nearest to the load, is designated as the measurement converter (assumed to be the 1st converter). This converter gathers voltage data from the grid and collects output current information from all converters. Then, the current sharing error for each converter is calculated as follows:

$$\Delta I_{o_i} = (N - 1) I_{o_i} - \sum_{k=1}^N (I_{o_j}) \quad (i \in N, j \neq i \in N) \quad (8)$$

Subsequently, V_{load} and ΔI_{o_i} are transmitted to other power converters through the communication link, facilitating coordinated operation and control across the system. In the second part, titled ‘Current Sharing and Load Voltage Controller’, the system’s controllers utilize input signals ($V_{load}, \Delta I_{o_i}$) to regulate output signals V_{adj_i}, R_{adj_i} . The adjustable virtual resistance R_{adj_i} is calculated as follows

$$R_{adj_i} = \Delta I_{o_i} K_{pRD} + \frac{1}{s} \Delta I_{o_i} K_{iRD} \quad (9)$$

where K_{pRD}, K_{iRD} are controller gains, and $(1/s) \Delta I_{o_i}$ represents the integration of current sharing error. To improve the voltage quality, the voltage shifting term V_{adj_i} is adaptively adjusted by the secondary controller, and its value is utilized to define the modified normal voltage variable:

$$\Delta V_{o_i} = (V_{nor_i} - V_{load}) \quad (10)$$

$$V_{nor_i}^* = (\Delta V_{o_i}) \left(K_{pV} + \frac{1}{s} K_{IV} \right) + V_{nor_i} = V_{adj_i} + V_{nor_i} \quad (11)$$

In the third part, termed ‘Modified Droop Controller’, the output voltage reference ($V_{o_i}^*$) of the supply controller for each module is determined by using the (12)

$$V_{o_i}^* = V_{nor_i}^* - I_{o_i} (R_{Droop} + R_{adj_i}) \quad (12)$$

In the fourth part, designated as ‘Primary Control Loop for i th Controller’, input signals ($V_{o_i}^*, V_{o_i}$) are processed to produce the PWM signal (Duty cycle) as the output signal for DC-DC converter. The function of this part involves the adoption of a voltage control loop, aided by a proportional integral controller, to regulate the output voltage of the i th converter, ensuring alignment with its designated output voltage reference $V_{o_i}^*$. This control approach facilitates proper voltage regulation and enhances the converter's current sharing within the DC system. The algorithm flow chart in Fig. 5 illustrates the sequence between control Parts in the Digital layer, aiding readers in visualizing the process step-by-step.

3.2. Primary control loop of the converter

To correctly control the output voltage of the converters, the primary control employs a cascade control structure, as shown in Fig. 4.

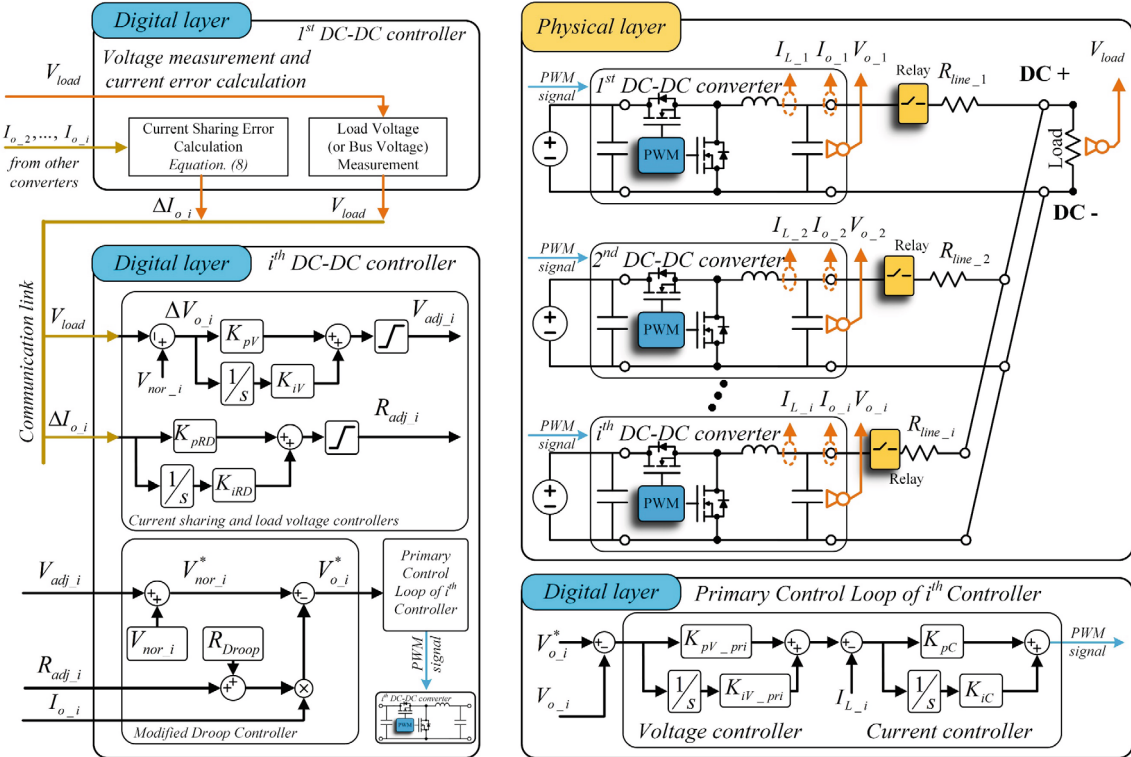


Fig. 4. Block diagram of the proposed control scheme with physical layer and digital layer

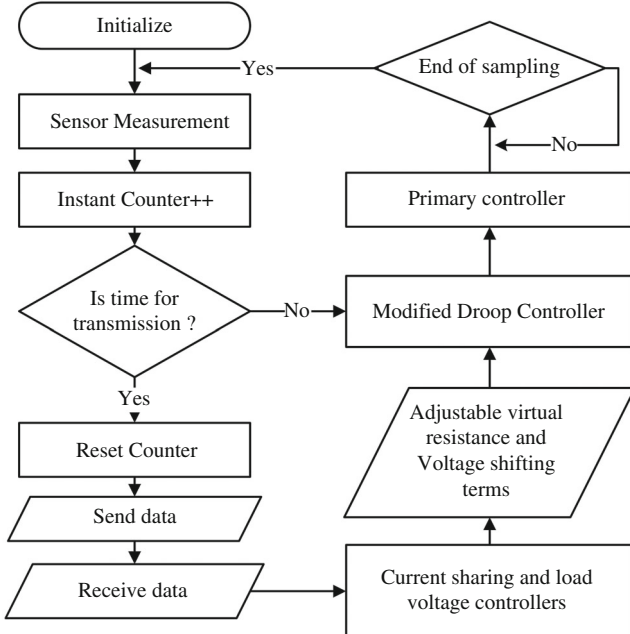


Fig. 5. Flowchart of the proposed control method

The cascade control structure comprises an outer voltage controller and an inner current controller [12], as shown below:

$$G_{V_pri}(s) = \frac{K_{pV_pri}s + K_{iV_pri}}{s} = \frac{1}{R_{Load}} + \frac{1}{\omega_1 R_{Load}} \frac{1}{s} \quad (13)$$

$$\begin{aligned} G_{C_pri}(s) &= \frac{K_{pC}s + K_{iC}}{s} \\ &= \frac{\omega_K^2 L(Ts + 1)}{V_{DC}s} = \frac{K^2 \omega_1^2 L(T_K s + 1)}{V_{DC}s}; T_K = \frac{2}{\omega_K} \end{aligned} \quad (14)$$

where $G_{V_pri}(s)$ is the proportional-integral controller for the voltage control loop; $\omega_1 = 1/(R_{Load}C)$, V_{DC} is the input source voltage; C is the capacitance value in the DC-DC buck converter; $G_{C_pri}(s)$ is the controller for the current control loop, in which L is the inductance value of the DC-DC buck converter; ω_1 and ω_K are angular frequencies the natural oscillation frequencies and current controller, respectively. In the studied system, $L = 330\mu H$ and $C = 940\mu F$. For the DC-DC converter, the bandwidth of the inner current control loop (ω_K) is set to be 10 times the outer voltage control loop (ω_1) to reduce the effect of noise components on the system response [13].

4. Simulation Results

In this study, we propose to simulate the proposed control scheme using MATLAB-SIMULINK software with two converter-based generators under various load conditions, as depicted in Fig. 6, with parameters outlined in Table I. To facilitate the assessment of controller efficiency, converter 2 only adopts a fixed droop gain, and the power from both sources is kept equal ($R_{Droop_1} = R_{Droop_2} = R_{Droop}$).

4.1. Conventional control scheme In the simulation scenario with a conventional control scheme, the conventional droop control scheme with a fixed initial electrical resistance value (R_{Droop}) is adopted in the microgrid system with only load 1. At

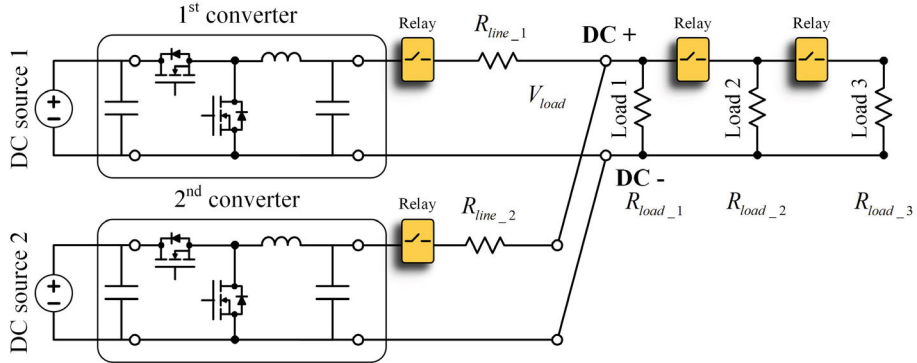


Fig. 6. Model schematic used in simulation

Table I. System parameters

Parameter	Value
Units of DC microgrid	
Load resistance 1,2 and 3 (R_{load_1} , R_{load_2} , R_{load_3})	4 Ω
Line resistance 1 (R_{line_1})	0.25 Ω
Line resistance 2 (R_{line_2})	0.75 Ω
Communication delay	10 ms
Ideal bus (load) voltage ($V_{nor_1} = V_{nor_2} = V_{nor}$)	48 V
Units of Primary control	
Proportional voltage gain (K_{pV_pri})	0.5
Intergal voltage gain (K_{iV_pri})	50
Proportional voltage gain (K_{iC})	0.01
Intergal current gain (K_{iC})	10
Units of Secondary control	
Proportional voltage gain (K_{pV})	0.75
Intergal voltage gain (K_{iV})	20
Proportional voltage gain (K_{pRD})	1
Intergal current gain (K_{iRD})	50
Units of Droop value	
Low Droop gain (R_{Droop})	0.5 Ω
High Droop gain (R_{Droop})	1 Ω

$t = 1$ s, load 2 is connected to the system to evaluate the voltage drop and current sharing performance.

Figure 7(a) and (b) show the output currents of two converters operating under the conventional control scheme, depicting scenarios with low and high droop gains. In the low droop gain case ($R_{Droop} = 0.5$), the current sharing error (ΔI_{o_1}) exhibits a noticeable value of 2.69 A at $t = 0.5$ s, which increases to 4.86 A (at $t = 2$ s) upon connection of load 2 to the system, as shown in Fig. 7(a). Conversely, in the high droop gain case ($R_{Droop} = 1$), the current sharing error (ΔI_{o_1}) is 1.69 A at $t = 0.5$ s, smaller than that of the low droop gain case (1.69 A < 2.69). However, this error still increases to 2.93 A at $t = 2$ s when load 2 is connected to the system, as shown in Fig. 7(b). Despite the distribution of load currents between two converters, the conventional droop control scheme fails to accurately share the output currents.

Figure 8(a) and 8(b) depict the voltage deviation (ΔV_{o_1}) with the conventional control scheme under low and high droop gain cases. To assess performance, the percentage deviation of voltage is defined as $error_{Vload}(\%) = \Delta V_{o_1}/V_{nor} \times 100\%$. In Fig. 8(a), the voltage drop in the DC bus increases from 10.448% (42.985 V, at $t = 0.5$ s) to 18.958% (38.9 V, at $t = 2$ s) when load 2 is connected to the system. In Fig. 8(b), the bus voltage deviation in the microgrid increases from 14.669% (40.959 V, at $t = 0.5$ s) to 26.669% (35.199 V, at $t = 2$ s).

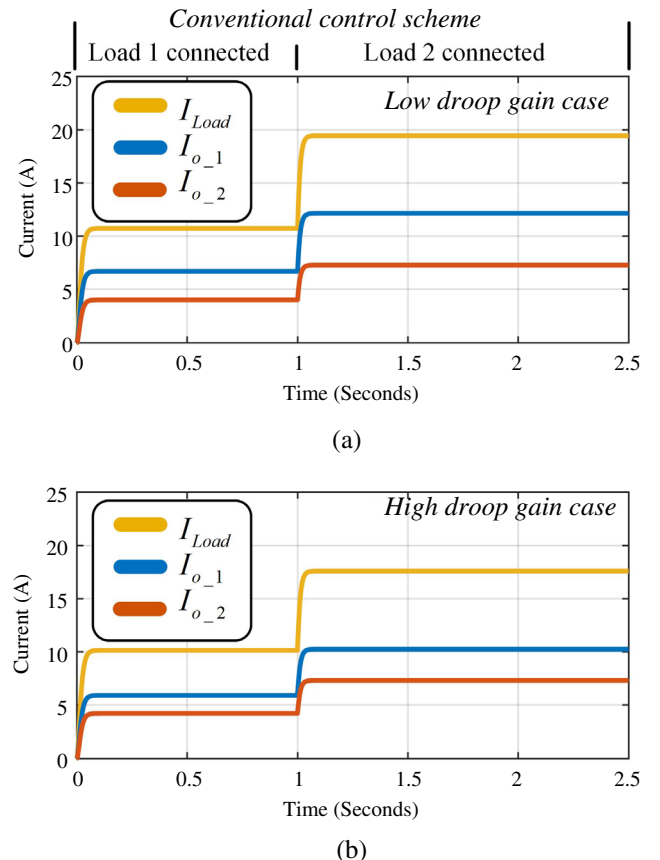


Fig. 7. Converter output currents with the conventional control scheme. (a) Low droop gain and (b) high droop gain

From Fig. 8(a) and (b), it is evident that microgrid voltage deviation is unavoidable with the conventional scheme, and this value tends to increase with increasing droop gain and load power demand. Based on the results from Figs. 7 and 8, inaccurate current sharing and high voltage deviation emerge as the primary issues of the conventional control method.

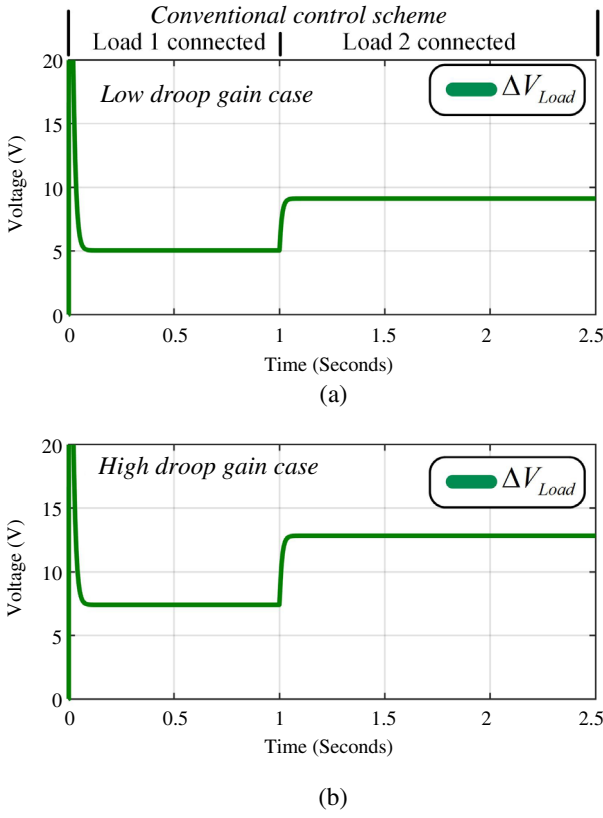


Fig. 8. The voltage deviation with conventional control scheme.
(a) Low droop gain and (b) high droop gain

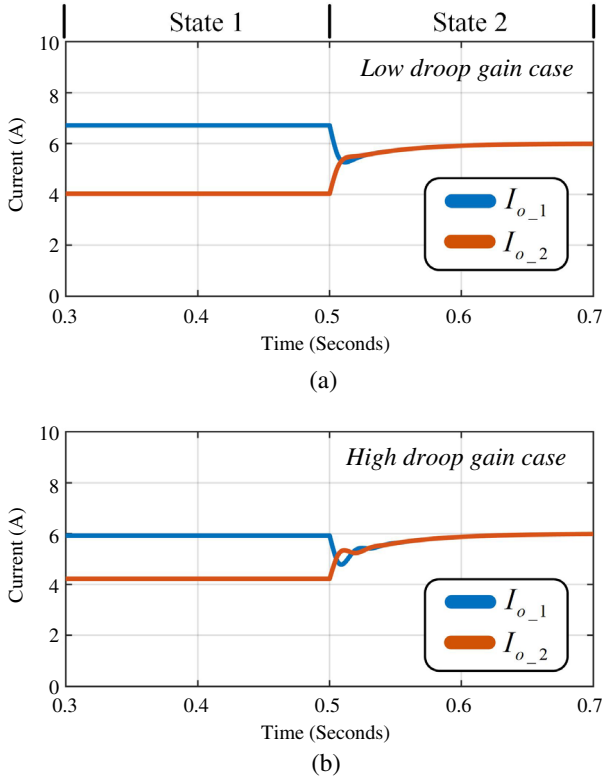


Fig. 9. Current sharing performance using the proposed adaptive control. (a) Low droop gain and (b) high droop gain

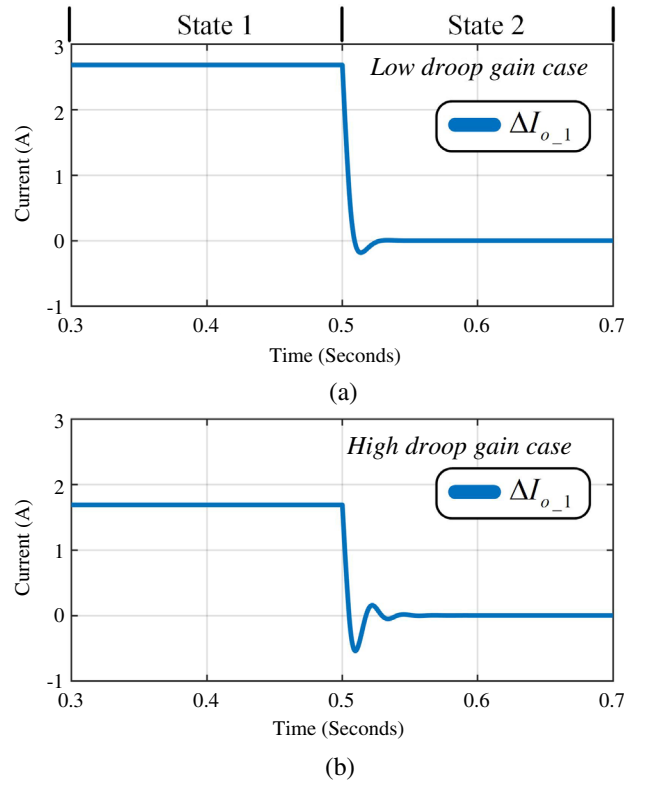


Fig. 10. Difference current between two converters. (a) Low droop gain and (b) high droop gain

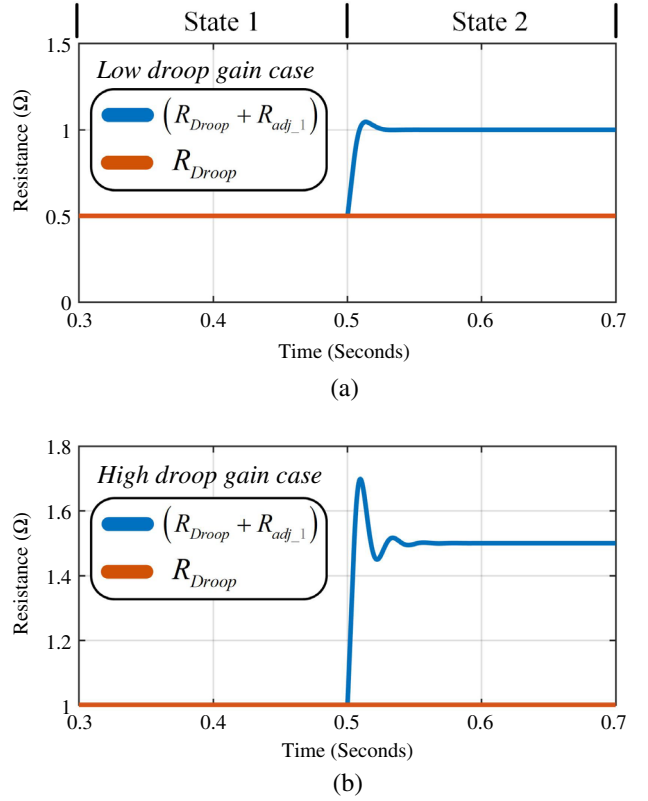


Fig. 11. Droop control variable in the proposed adaptive control method. (a) Low droop gain and (b) high droop gain

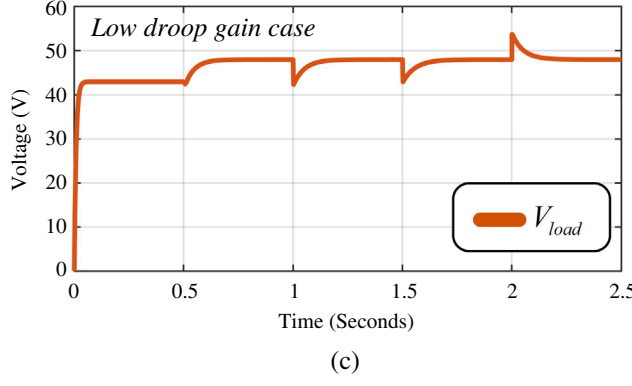
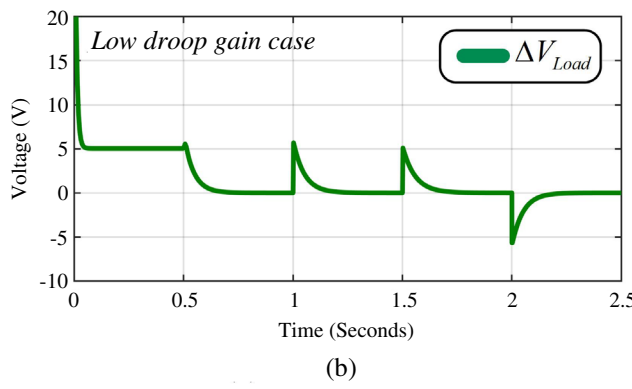
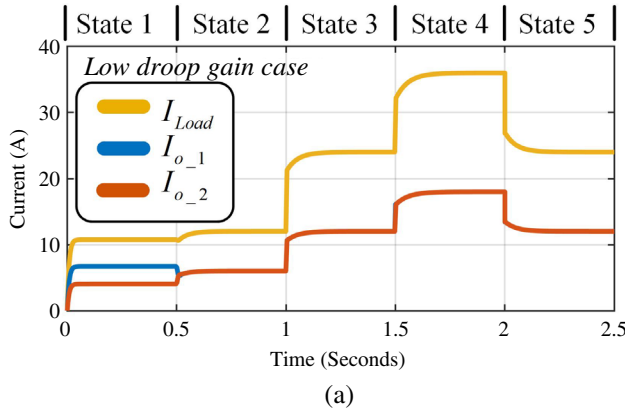


Fig. 12. The output currents, voltage deviation, and load (bus) voltage under different load conditions with low droop gain. (a) Output currents, (b) voltage deviation and (c) DC bus voltage

4.2. Proposed adaptive current sharing and voltage deviation minimized

This simulation scenario with the proposed control scheme is divided into five states:

State 1 ($t < 0.5s$): The conventional droop control scheme is adopted with a fixed initial electrical resistance value.

State 2 ($0.5s \leq t < 1s$): the proposed control scheme with adjustable resistance and voltage shifting term is enabled.

State 3 ($1s \leq t < 1.5s$): load 2 is connected to the system to evaluate the proposed control performance.

State 4 ($1.5s \leq t < 2s$) and State 5 ($2s \leq t < 2.5s$): load 3 is subsequently connected to and disconnected from the system to evaluate the proposed control performance.

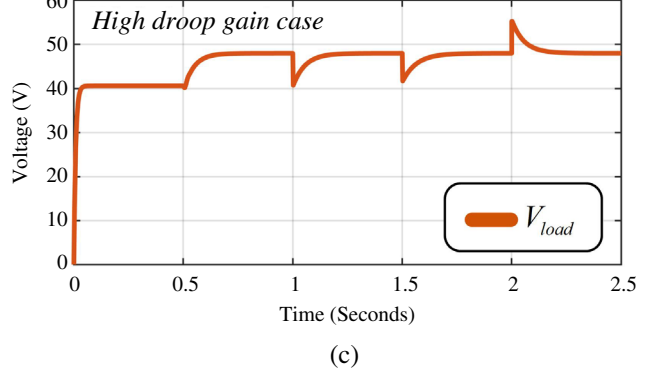
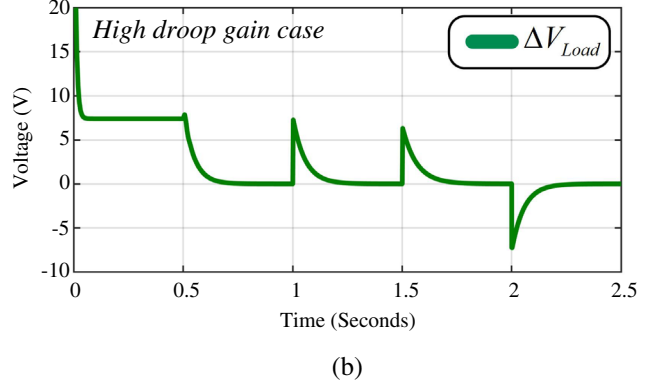
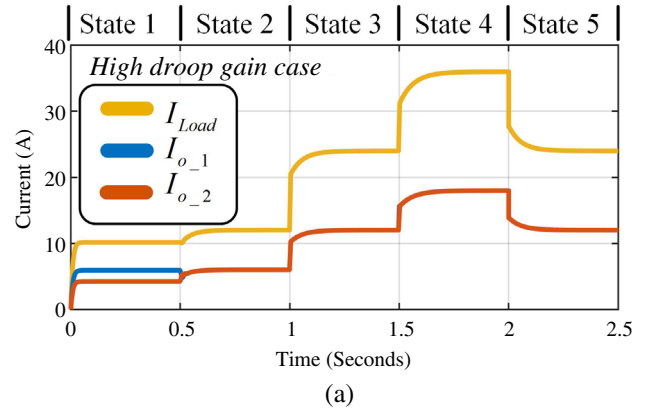


Fig. 13. The output currents, voltage deviation, and load (bus) voltage under different load conditions with high droop gain. (a) Output currents, (b) voltage deviation and (c) DC bus voltage

The choice to double and triple the load power demand ($R_{load_3} = R_{load_2} = R_{load_1}$) in this study aims to assess the reliability and performance of the controller under extreme scenarios. The current sharing performance of the proposed control scheme is depicted in Fig. 9(a) for states 1 and 2 under the low droop gain case, and in Fig. 9(b) under the high droop gain case.

Before the proposed control scheme is activated, the current sharing error is notably high at 2.69 A at $t = 0.4$ s in the low droop gain case. By enabling the proposed control scheme at $t = 0.5$ s, the current sharing error is reduced gradually, reaching a small value of 0.01 A at the steady state by $t = 0.7$ s. Similarly, in the high droop gain case, the current sharing error decreases from 1.69 A (at $t = 0.4$ s) prior to the activation of the proposed controller to

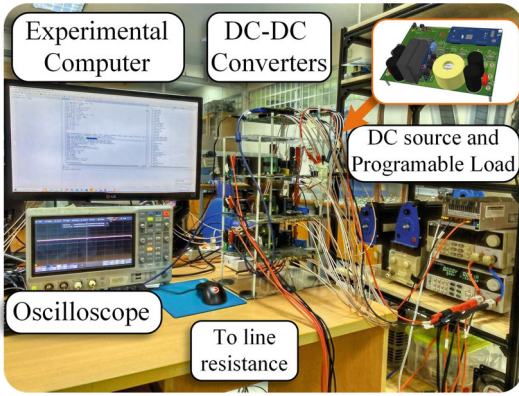


Fig. 14. The small-scale laboratory experimental system.

0.01 A (at $t = 0.7$ s) after its implementation. The corresponding current sharing error under low and high droop gain cases are shown in Fig. 10(a) and (b).

Figure 11(a) and (b) illustrate the dynamic of R_{Droop} and $R_{Droop} + R_{adj_1}$ under high and low droop gain cases. Initially, $R_{adj_1} = 0$ in state 1 ($t < 0.5$ s), while R_{Droop} is set to the default values of high and low droop cases. In cases where the shared current between the two converters is unequal, the adjustable resistance R_{adj_1} is regulated to improve the current sharing accuracy.

In the steady state under low droop gain case, $(R_{Droop} + R_{adj_1})$ increases from 0.5Ω to 1Ω , as illustrated in Fig. 11(a). Similarly, in the high droop gain case, $(R_{Droop} + R_{adj_1})$ increases from 1Ω to over 1.5Ω , as shown in Fig. 11(b).

Figure 12 shows output currents, load voltage deviation, and load voltage under different load conditions, specifically when the load is doubled or tripled from its initial low power level, under the low droop gain case. The simulation results in Fig. 12(a) and (b) indicate that the proposed control scheme has properly shared the current between the two converters, with a deviation of load voltage is 0.01% and a small current sharing error (0.01A) observed in the steady state (at $t = 0.75$ s, 1.25 s, 1.75 s, and 2.25 s).

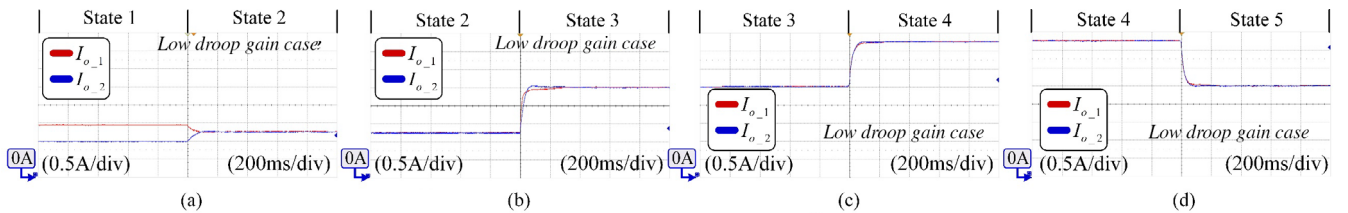


Fig. 15. The experimental results of output currents under different load conditions in the low droop gain case. (a) During State 1–State 2, (b) During State 2–State 3, (c) During State 3–State 4 and (d) During State 4–State 5

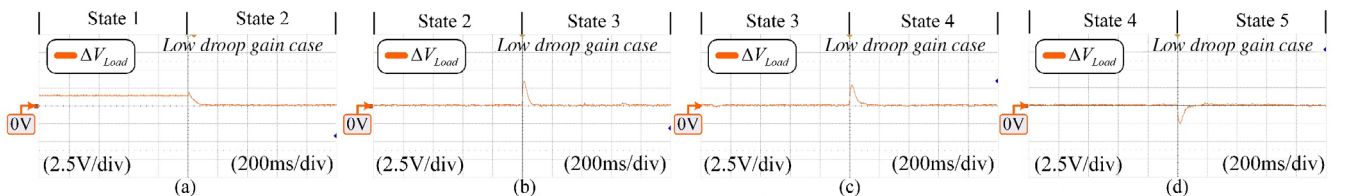


Fig. 16. The experimental results of load voltage deviation under different load conditions in the low droop gain case. (a) During State 1–State 2, (b) During State 2–State 3, (c) During State 3–State 4 and (d) During State 4–State 5

Whenever the load changes, the proposed controller compensates for the voltage drop and mismatched current sharing even though load 2 and load 3 are respectively connected to the microgrid at $t = 1$ s, $t = 1.5$ s, and $t = 2$ s. Consequently, the load voltage is restored to its nominal value of 48 V across various load conditions, as depicted in Fig. 12(c).

Figure 13(a)–(c) presents the output currents, voltage deviation, and load voltage under different load conditions in the high droop gain case. Similarly, the proposed control method adeptly regulates voltage shifting terms to minimize microgrid voltage deviation and adjusts current sharing to enhance system reliability. Consequently, despite load variations, the load voltage is maintained at the desired value in the high droop gain case.

The simulation results in Figs. 12 and 13 demonstrate the robustness of the proposed control scheme in achieving accurate current sharing and minimizing voltage deviation under various load conditions and droop gain values. This highlights its effectiveness in ensuring stable operation and reliability of the system.

5. Experimental Validation

Figure 14 illustrates the small-scale experimental setup in the laboratory. This experimental system is characterized by the following laboratory parameters: $V_{nor_1} = V_{nor_2} = 48V$, the emulated communication delay is 10 ms, $R_{line_1} = 0.5\Omega$, $R_{line_2} = 1\Omega$, the low droop gain case is considered with $R_{Droop} = 0.5\Omega$, and the load resistances are selected as $R_{load_1} = R_{load_2} = R_{load_3} = 20\Omega$.

Figures 15–17 show the experimental results of output currents, voltage deviation, and load voltage, under the low droop gain case. With the implementation of our proposed control scheme in State 2, the controller effectively compensates for current-sharing mismatches and reduces voltage deviation to a small value, as shown in Figs. 15 and 16. Consequently, the quality of the DC bus voltage is enhanced with load voltage maintained at the desired normal value, as shown in Fig. 17.

Furthermore, throughout load 2 connections in State 3 and subsequent load 3 connect-disconnect sequences in States 4 and 5, the proposed system maintains consistent control performance

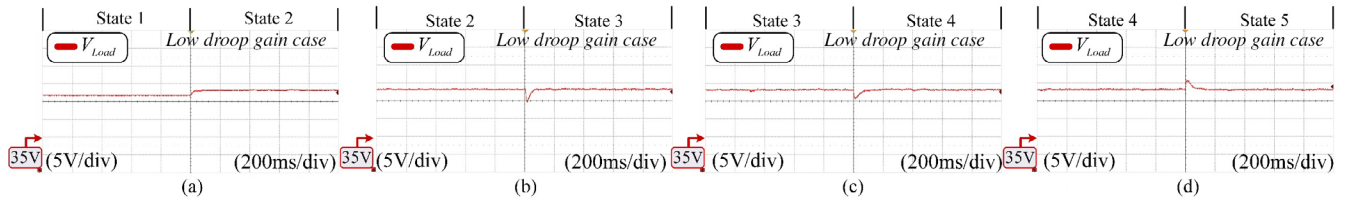


Fig. 17. The experimental results of load voltage under different load conditions in the low droop gain case. (a) During State 1–State 2, (b) During State 2–State 3, (c) During State 3–State 4 and (d) During State 4–State 5

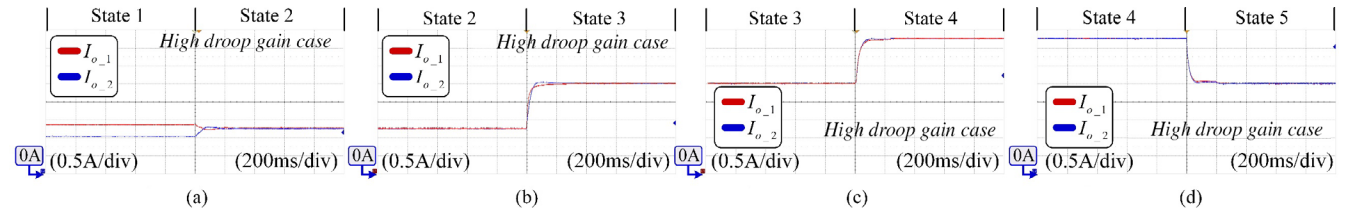


Fig. 18. The experimental results of output currents under different load conditions in the high droop gain case. (a) During State 1–State 2, (b) During State 2–State 3, (c) During State 3–State 4 and (d) During State 4–State 5

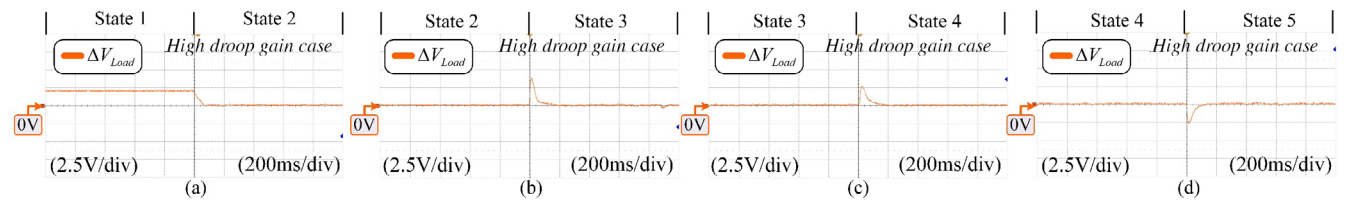


Fig. 19. The experimental results of load voltage deviation under different load conditions in the high droop gain case. (a) During State 1–State 2, (b) During State 2–State 3, (c) During State 3–State 4 and (d) During State 4–State 5

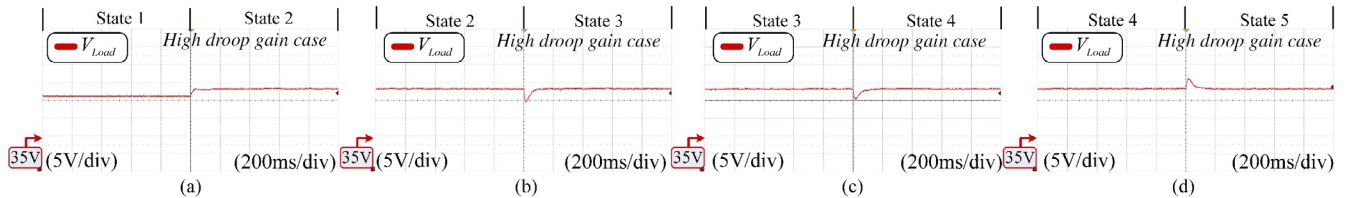


Fig. 20. The experimental results of load voltage under different load conditions in the high droop gain case. (a) During State 1–State 2, (b) During State 2–State 3, (c) During State 3–State 4 and (d) During State 4–State 5

and reliability. The load voltage waveform in Fig. 17 confirms the advantage of the proposed controller in regulating and maintaining the load voltage at normal (ideal) voltage value.

Figures 18–20 show the experimental results of output currents, voltage deviation, and load voltage under the high droop gain case. Similar to the low droop gain case, the proposed controller effectively regulates the output current of both converters to the desired value, as shown in Fig. 18. Additionally, Figs. 19 and 20 show the output voltage of each converter is appropriately adjusted to ensure that the load voltage remains within the normal range, thereby minimizing load voltage deviation.

6. Conclusion

In conclusion, the proposed control scheme offers a simple and effective solution for addressing voltage quality and current-sharing concerns in distributed DC-DC converter systems. By regulating the adjustable resistance and compensating for voltage deviation, this approach ensures proper current sharing and load voltage quality without extensive parameter knowledge. Sim-

ulations and laboratory experiments demonstrate consistent performance in maintaining accurate current sharing and minimizing voltage deviation under varying load conditions, even when the load power demand doubles or triples. The proposed system exhibits stable performance even during load connect-disconnect sequences and under both low and high droop gain cases, showcasing its feasibility and reliability in practice.

Acknowledgments

We acknowledge Ho Chi Minh City University of Technology (HCMUT), VNU-HCM for supporting this study.

References

- (1) Sepulveda NA, Jenkins JD, Edington A, Mallapragada DS, Lester RK. The design space for long-duration energy storage in decarbonized power systems. *Nature Energy* 2021; **6**(5):506–516. <https://doi.org/10.1038/s41560-021-00796-8>.
- (2) Michalski J, Poltrum M, Bünger U. The role of renewable fuel supply in the transport sector in a future decarbonized energy system. *Inter-*

- national Journal of Hydrogen Energy* 2019; **44**(25):12554–12565. <https://doi.org/10.1016/j.ijhydene.2018.10.110>.
- (3) Saeed MH, Fangzong W, Kalwar BA, Iqbal S. A review on Microgrids' challenges & perspectives. *IEEE Access* 2021; **9**:166502–166517. <https://doi.org/10.1109/ACCESS.2021.3135083>.
 - (4) Al-Ismail FS. DC microgrid planning, operation, and control: A comprehensive review. *IEEE Access* 2021; **9**:36154–36172. <https://doi.org/10.1109/ACCESS.2021.3062840>.
 - (5) Abhishek A, Ranjan A, Devassy S, Kumar Verma B, Ram SK, Dhakar AK. Review of hierarchical control strategies for DC microgrid. *IET Renewable Power Generation* 2020; **14**(10):1631–1640. <https://doi.org/10.1049/iet-rpg.2019.1136>.
 - (6) Espina E, Llanos J, Burgos-Mellado C, Cárdenas-Dobson R, Martínez-Gómez M, Sáez D. Distributed control strategies for microgrids: An overview. *IEEE Access* 2020; **8**:193412–193448. <https://doi.org/10.1109/ACCESS.2020.3032378>.
 - (7) Prabhakaran P, Goyal Y, Agarwal V. Novel nonlinear droop control techniques to overcome the load sharing and voltage regulation issues in DC microgrid. *IEEE Transactions on Power Electronics* 2018; **33**(5):4477–4487. <https://doi.org/10.1109/TPEL.2017.2723045>.
 - (8) Mehdi M, Kim CH, Saad M. Robust centralized control for DC islanded microgrid considering communication network delay. *IEEE Access* 2020; **8**:77765–77778. <https://doi.org/10.1109/ACCESS.2020.2989777>.
 - (9) Peng J, Fan B, Liu W. Voltage-based distributed optimal control for generation cost minimization and bounded bus voltage regulation in DC microgrids. *IEEE Transactions on Smart Grid* 2021; **12**(1):106–116. <https://doi.org/10.1109/TSG.2020.3013303>.
 - (10) Lin Y, Xiao W. Novel piecewise linear formation of droop strategy for DC microgrid. *IEEE Transactions on Smart Grid* 2019; **10**(6):6747–6755. <https://doi.org/10.1109/TSG.2019.2911013>.
 - (11) Peyghami S, Davari P, Mokhtari H, Blaabjerg F. Decentralized droop control in DC microgrids based on a frequency injection approach. *IEEE Transactions on Smart Grid* 2019; **10**(6):6782–6791. <https://doi.org/10.1109/TSG.2019.2911213>.
 - (12) Tsang KM, Chan WL. Cascade controller for DC/DC buck converter. *IEE Proceedings: Electric Power Applications* 2005; **152**(4):827–831. <https://doi.org/10.1049/ip-epa:20045198>.
 - (13) Wang L, Liu X, Ni X, Jiang S, Liu S. A stability control way of bus voltage in DC microgrid with constant power load. *IEEJ Transactions on Electrical and Electronic Engineering* 2021; **16**(9):1187–1194. <https://doi.org/10.1002/tee.23416>.

Hong Phuc Lam (Non-member) is a researcher at Faculty of Electrical and Electronic Engineering, Ho Chi Minh City University of Technology, Vietnam. His research interests include control theory, power electronics, system identification, and smart grid.



Quang T. D. Pham (Non-member) is a lecturer at the Faculty of Transportation Engineering, Ho Chi Minh City University of Technology (HCMUT), Vietnam National University Ho Chi Minh City (VNU-HCM), Vietnam. He received a M.Sc. degree in 2019. His current research interests include Vehicle Maintenance, Self-Driving Car, Computational Fluid Dynamics (CFD), DC-DC converter.



Thoi Hung Ly (Non-member) is a researcher at Faculty of Electrical and Electronic Engineering, Ho Chi Minh City University of Technology, Vietnam. His research interests include control theory, power electronics, system identification, and smart grid.



Minh Duc Pham (Non-member) received the Master and Ph.D. degrees in Electrical Engineering from Ulsan University, South Korea. He is currently a full-time lecturer at Ho Chi Minh City University of Technology, Vietnam. His research interests include Hybrid AC-DC microgrids, PMSM, low-cost inverters, and renewable energy.



Duc Hung Nguyen (Non-member) received the B.E.(2004), and M.E. (2009) degrees in electrical engineering from Ho Chi Minh City University of Technology, Vietnam. His research interests include power electronics, electrical machine drives, low-cost inverter, and renewable energy, OBC.

